Original Article | Nuclear Medicine

http://dx.doi.org/10.3348/kjr.2015.16.4.919
pISSN 1229-6929 · eISSN 2005-8330
Korean J Radiol 2015;16(4):919-928

Korean Journal of Radiology
KJR

Detection of Myocardial Metabolic Abnormalities by 18F-FDG PET/CT and Corresponding Pathological Changes in Beagles with Local Heart Irradiation

Rui Yan, MM[1, 2], Jianbo Song, MM[2], Zhifang Wu, MD[2], Min Guo, MD[3], Jianzhong Liu, MM[2], Jianguo Li, MM[4], Xinzhong Hao, MM[2], Sijin Li, MD[2]

[1]Nursing College of Shanxi Medical University, Taiyuan 030001, China; Departments of [2]Nuclear Medicine and [3]Cardiology, First Hospital of Shanxi Medical University, Taiyuan 030001, China; [4]Department of Radiological and Environmental Medicine, China Institute for Radiation Protection, Taiyuan 030006, China

Objective: To determine the efficacy of 18F-fluorodeoxyglucose positron emission tomography/computed tomography (18F-FDG PET/CT) in the detection of radiation-induced myocardial damage in beagles by comparing two pre-scan preparation protocols as well as to determine the correlation between abnormal myocardial FDG uptake and pathological findings.

Materials and Methods: The anterior myocardium of 12 beagles received radiotherapy locally with a single X-ray dose of 20 Gy. 18F-FDG cardiac PET/CT was performed at baseline and 3 months after radiation. Twelve beagles underwent two protocols before PET/CT: 12 hours of fasting (12H-F), 12H-F followed by a high-fat diet (F-HFD). Regions of interest were drawn on the irradiation and the non-irradiation fields to obtain their maximal standardized uptake values (SUVmax). Then the ratio of the SUV of the irradiation to the non-irradiation fields (INR) was computed. Histopathological changes were identified by light and electron microscopy.

Results: Using the 12H-F protocol, the average INRs were 1.18 ± 0.10 and 1.41 ± 0.18 before and after irradiation, respectively (p = 0.021). Using the F-HFD protocol, the average INRs were 0.99 ± 0.15 and 2.54 ± 0.43, respectively (p < 0.001). High FDG uptake in irradiation field was detected in 33.3% (4/12) of 12H-F protocol and 83.3% (10/12) of F-HFD protocol in visual analysis, respectively (p = 0.031). The pathology of the irradiated myocardium showed obvious perivascular fibrosis and changes in mitochondrial vacuoles.

Conclusion: High FDG uptake in an irradiated field may be related with radiation-induced myocardial damage resulting from microvascular damage and mitochondrial injury. An F-HFD preparation protocol used before obtaining PET/CT can improve the sensitivity of the detection of cardiotoxicity associated with radiotherapy.

Index terms: *18F-FDG PET/CT; Radiation-induced heart disease; Radiotherapy; Pathology*

Received October 14, 2014; accepted after revision April 24, 2015.
This study was supported by grants from the Natural Science Foundation of China (No. 81171374) and Natural Science Foundation for Young Scientists of Shanxi Province, China (No. 2013021035-2).

Corresponding author: Sijin Li, MD, Department of Nuclear Medicine, First Hospital of Shanxi Medical University, No. 85, Jiefang Road, Taiyuan, Shanxi 030001, China.
• Tel: (86351) 4639278 • Fax: (86351) 4048123
• E-mail: lisj_nm1@sohu.com

INTRODUCTION

Radiation-induced heart disease (RIHD) is a serious side effect of radiotherapy (RT) of thoracic tumors when all or part of the heart is included in the irradiation field. A meta-analysis conducted by the Early Breast Cancer Trialists' Collaborative Group found a higher cardiac mortality rate in patients who received RT (1). Aleman et al. (2) reported that the incidence of congestive heart failure and myocardial infarction in Hodgkin's lymphoma patients who received RT was significantly higher than that in the normal population. Other studies have reported that survivors of

lung cancer (3, 4) and esophageal cancer (5) tend to have an increased incidence of heart disease or reduction in the ejection fraction after irradiation. Although advances in RT techniques have reduced the exposure dose and volume of the heart, cardiotoxicity has not been eliminated (6, 7). Hence, RIHD could potentially offset the benefit of RT for long-term cancer survivors. Therefore, it is particularly important to monitor and evaluate of RIHD after thoracic RT.

18F-fluorodeoxyglucose positron emission tomography/computed tomography (18F-FDG PET/CT) is valuable for evaluating tumor extension or detecting recurrence in patients with thoracic tumors (8). It is an important noninvasive technique for follow-up after chemoradiotherapy for thoracic tumors. Several studies have found that focal increased 18F-FDG uptake in the irradiation field is sometimes seen in patients with thoracic tumors after RT (9-11). We suspected that abnormal 18F-FDG uptake might be related to RIHD. However, the value of 18F-FDG PET for the diagnosis of RIHD has not been fully explored. Previous clinical studies have almost been retrospective in nature, and in these studies 18F-FDG PET was not performed before RT. Thus, increased 18F-FDG uptake may have already been evident before RT. In addition, almost all of the cancer patients in these studies were irradiated with concurrent chemotherapy, and some patients were at high risk for cardiovascular, disease or diabetes mellitus. These multiple confounding factors may cause the unclearness of the impact have caused an unclear effect of RT on changes in myocardial metabolism. Furthermore, frequent variable physiological myocardial FDG uptake is the major limitation of PET examinations. As previously reported, a diffuse myocardial 18F-FDG uptake pattern even under fasting conditions is common (12, 13). Thus, whether focal increased 18F-FDG uptake is related to RIHD is unclear. In addition, the correlations between 18F-FDG-PET findings and pathology are unknown.

Therefore, in the present study, we investigated cardiac 18F-FDG uptake findings after radiation, as well as the pathology of those changes in a beagle model of regional heart irradiation.

MATERIALS AND METHODS

Animals and Experimental Schemes

All of the study protocols were approved by our Institutional Animal Care and Use Committee and were performed in accordance with the Guidelines for Animal Experiments of Shanxi Medical University.

Twelve male adult beagle dogs (weight range: 11–15 kg) were obtained from Anhui Fuyang Weiguan Institute of Experimental Animals. The Dogs were housed at Experimental Animal Center of the Chinese Academy of Radiation Medicine and Protection Institute at a temperature of 18–25°C and humidity of 40–60%, and were fed with commercial diets and tap water *ad libitum*.

18F-FDG cardiac PET/CT and echocardiography were performed at baseline and 3 months after irradiation. All of the animals were scarified 1 week after all of the examinations. Each animal's heart was subjected to pathological testing by light and electron microscopy.

Animal Model of Regional Heart Irradiation

Anesthetized dogs (pentobarbital, 30 mg/kg) were shielded with lead plates leaving the thorax region exposed. The left ventricular anterior wall was outlined as the RT target. The targeted volume accounted for 1/4 to 1/3 of the left ventricular volume. All of the animals received intensity-modulated RT with a single 20 Gray (Gy) dose. RT was delivered using a 6 MV X-ray system with a linear accelerator (Clinac IX: Varian Medical Systems, Palo Alto, CA, USA). Treatment planning was performed by computed tomography (CT) in all of the animals, and the dose distribution was determined using the Varian Medical Systems' Eclipse Treatment Planning System. The target area was verified by cone-beam CT scanning.

Preparation Protocols before PET/CT

All of the dogs underwent 18F-FDG PET/CT according to two preparation protocols, separated by 2–3 days: 12 hours of fasting before 18F-FDG tracer injection (12H-F), and 12 hours of fasting followed by a high-fat diet (HFD) followed another 3 hours before 18F-FDG tracer injection (F-HFD) (Fig. 1). The HFD consisted of fat (> 40%) and fiber (< 10%), with each dog consuming 105 ± 15 g.

18F-FDG Cardiac PET/CT

PET was performed 40–60 minutes after the administration of 18F-FDG at a dose of 3.7–5.5 MBq/kg using a Discovery VCT PET/CT (GE Healthcare, Waukesha, WI, USA) under conditions of the 12H-F or F-HFD protocol. The heart was localized using CT Scout imaging and PET/CT scanning using 1 PET bed width (15 cm) and taking the heart as the center. CT was performed first with using

Korean Journal of Radiology
KJR

the following parameters: a tube voltage of 120 kV, a tube current of 30 mA, and layers of 5 mm in height. Next, an electrocardiography-gated three-dimensional model was used to perform PET data collection (8 time phases per cardiac cycle). The data acquisition time was 10 min (matrix, 128 x 28; iterative reconstruction, 2; 20 subsets; half-height weight, 6 mm). CT data from the same scanner were used for attenuation correction, image reconstruction and merging of the PET image.

18F-FDG Image Interpretation

Before RT, inhibition of physiological myocardial 18F-FDG uptake by two prescan protocols was judged by two experienced observers visually and also quantitatively by measuring the maximal standardized uptake value (SUVmax) of the left ventricular myocardium. For the qualitative visual estimation of 18F-FDG myocardial uptake, 18F-FDG PET/CT scans were divided into four grades as referenced by Williams and Kolodny (14): 0, homogeneously minimal; 1, mostly minimal or mild uptake; 2, mostly intense or moderate uptake; and 3, homogeneously intense (Fig. 2). Grade 0 can be recognized as complete inhibition of physiological myocardial uptake.

After RT, cases with higher 18F-FDG uptake in the myocardium (corresponding to the irradiated field) than in other areas were diagnosed as positive findings; otherwise they were deemed negative with the agreement of two observers. In addition, 18F-FDG uptake in irradiated fields was also judged quantitatively by measuring SUVmax in the regions of interest (ROIs) drawn manually on the transaxial slices of PET images of the irradiated and non-irradiated fields of the myocardium with the assistance of radiotherapy-planning images. To reduce artificial error in the drawing of ROIs, we drew the ROIs of the irradiated and non-irradiated fields on the CT images and compared them to those on RT-simulation CT on the slice of the inferior vena cava entrance level, and then copied the ROIs to PET images to obtain each SUVmax. Then the ratio of the SUV of the irradiation field to the non-irradiation field (irradiation to non-irradiation ratio, INR) was computed. Volumetrix software running on a GE Xerleris workstation (GE Healthcare) was used to interpret the data.

Echocardiography

An SSH 880CV Doppler echocardiograph (Toshiba Medical Systems, Otawara, Japan) with a 3-MHz flat plane arrow probe (PST-30BT) was used. Examination was performed by one experienced investigator. The left ventricular end-systolic diameter (LVEDs) and left ventricular end-diastolic diameters (LVEDd) were measured by M-mode echocardiography. Mitral valve diastolic waves (E waves, A waves, E/A ratio) were also calculated using Doppler studies. The LV ejection fraction (LVEF) was calculated using a modified Simpson's method.

Histopatholgic Evaluation

After all of the animals underwent the above examinations, the dogs were sacrificed by the acute blood loss method after anesthetization with 3% pentobarbital. The chest of each dog was opened; before the heart

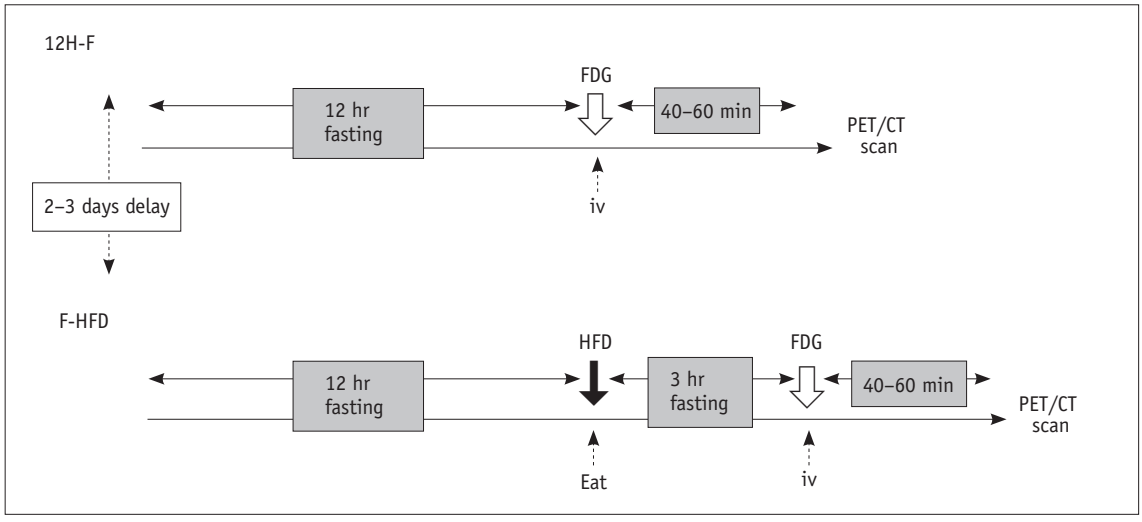

Fig. 1. Description of two preparation protocols. 12H-F = 12 hours of fasting, FDG = fluorodeoxyglucose, F-HFD = fasting followed by a high-fat diet, HFD = high-fat diet, PET/CT = positron emission tomography/computed tomography

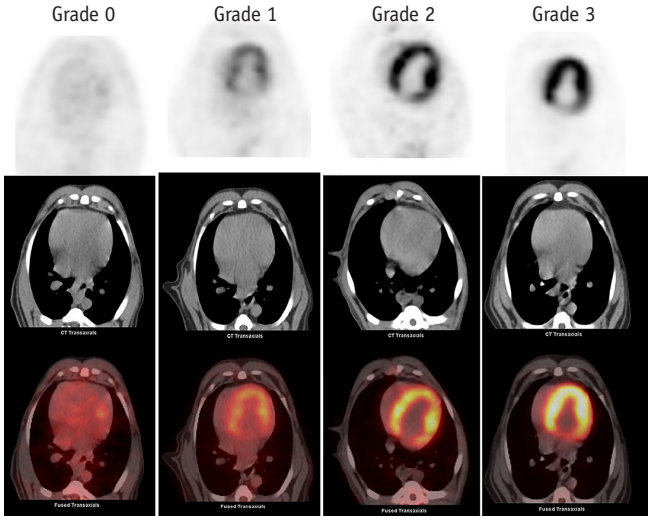

Fig. 2. 18F-FDG cardiac PET/CT images before RT from beagles treated with two pre-scan preparations. Grade 0 image from M4 using F-HFD protocol shows homogeneously minimal myocardial FDG uptake; Grade 1 image from M3 using F-HFD protocol shows mostly minimal or mild myocardial FDG uptake; Grade 2 image from M10 using 12H-F protocol shows mostly intense or moderate myocardial FDG uptake; Grade 3 image from M2 using 12H-F protocol shows homogeneously intense myocardial FDG uptake. 12H-F = 12 hours of fasting, 18F-FDG = 18F-fluorodeoxyglucose, F-HFD = fasting followed by a high-fat diet, PET/CT = positron emission tomography/computed tomography, RT = radiotherapy

Table 1. Myocardial FDG Uptake before RT Using 12H-F or F-HFD Protocol

12H-F Protocol	F-HFD Protocol				Total
	Grade 0	Grade 1	Grade 2	Grade 3	
Grade 0	3	1	0	0	4
Grade 1	1	0	0	0	1
Grade 2	4	1	0	0	5
Grade 3	2	0	0	0	2
Total	10	2	0	0	12

Date are presented as number; Grades 0–3 refer to qualitative visual estimation of FDG myocardial uptake: Grade 0, homogeneously minimal; Grade 1, mostly minimal or mild uptake; Grade 2, mostly intense or moderate uptake; Grade 3, homogeneously intense. 12H-F = 12-hour fasting before 18F-FDG tracer injection, 18F-FDG = 18F-fluorodeoxyglucose, F-HFD = 12-hour fasting followed by high fat diet and followed by another 3 hours before FDG tracer injection, RT = radiotherapy

stopped beating, and samples (1 mm^3) were cut from the posterior and anterior wall of left ventricular tissue; these were immediately fixed in 2.5% glutaraldehyde for electron microscopy. Next, the heart was removed and rinsed with saline, and then samples from the posterior and anterior wall of the left ventricular tissue were prepared for histological evaluation after fixation in 10% formalin solution. The sections were subjected to a graded alcohol dehydration process and were embedded in paraffin blocks, and sections (5 μm thick) were prepared for hematoxylin and eosin (H&E) staining. For electron microscopy, myocardial specimens were fixed in 2.5% glutaraldehyde and then were rinsed three times in phosphate buffer. After dehydration with ethanol and acetone, the specimens were embedded in epoxy resin. Ultrathin sections (50 nm) were cut from each sample, stained with uranium acetate and lead citrate, and examined with a transmission electron microscope (JEM-2100; JEOL Company, Tokyo, Japan) by two observers unaware of the treatments.

Statistical Analysis

The results were expressed as means ± standard deviations or numbers. Measurement data between groups were compared using paired Student's *t* test. Comparison of the proportion was made using the McNemar's test. The SPSS 13.0 software (SPSS Inc., Chicago, IL, USA) was used for statistical analysis. A *p* value less than 0.05 was deemed to indicate statistical significance.

RESULTS

Animal Condition

All of the dogs completed and survived the experimental procedure. No symptoms of heart failure were observed after RT. No significant differences were found in heart rates (132.4 ± 15.8 vs. 128.7 ± 16.0; $p = 0.633$), blood systolic pressure (159.2 ± 12.8 mm Hg vs. 160.7 ± 13.0 mm Hg; $p = 0.772$) and blood diastolic pressure (107.9 ± 9.4 mm Hg vs. 109.4 ± 13.3 mm Hg; $p = 0.771$) at baseline and 3 months after RT, respectively.

Inhibition of Physiological Myocardial 18F-FDG Uptake

Visual qualitative analysis revealed that 10 of 12 animals had grade 0 myocardial 18F-FDG uptake using the F-HFD protocol. However, only 4 of 12 animals had grade 0 myocardial 18F-FDG uptake or complete inhibition of the uptake using the 12H-F protocol (Table 1).

The SUVmax of the myocardium was significantly lower with the F-HFD protocol than with the 12H-F protocol (3.01 ± 1.59 vs. 8.27 ± 3.75, respectively; $p = 0.002$).

Detection of RIHD by 18F-FDG PET/CT

No abnormal 18F-FDG uptake in the myocardium was found before RT. However, 3 months after RT, high 18F-FDG uptake in the anterior myocardium corresponding to the

Korean Journal of Radiology
KJR

irradiated field was observed compared to outside of the irradiated field (Fig. 3). Cases with higher 18F-FDG uptake in the irradiated field than in other areas were diagnosed as positive; otherwise, the cases were deemed to be as negative. The F-HFD protocol detected a more positive rate than did the 12H-F protocols (10/12 vs. 4/12, respectively; $p = 0.031$; McNemar test) (Fig. 4, Table 2).

Using the 12H-F protocol, the average INRs before and after RT were 1.18 ± 0.10 and 1.41 ± 0.18, respectively ($p = 0.021$). Using the F-HFD protocol, the INRs were 0.99 ± 0.15

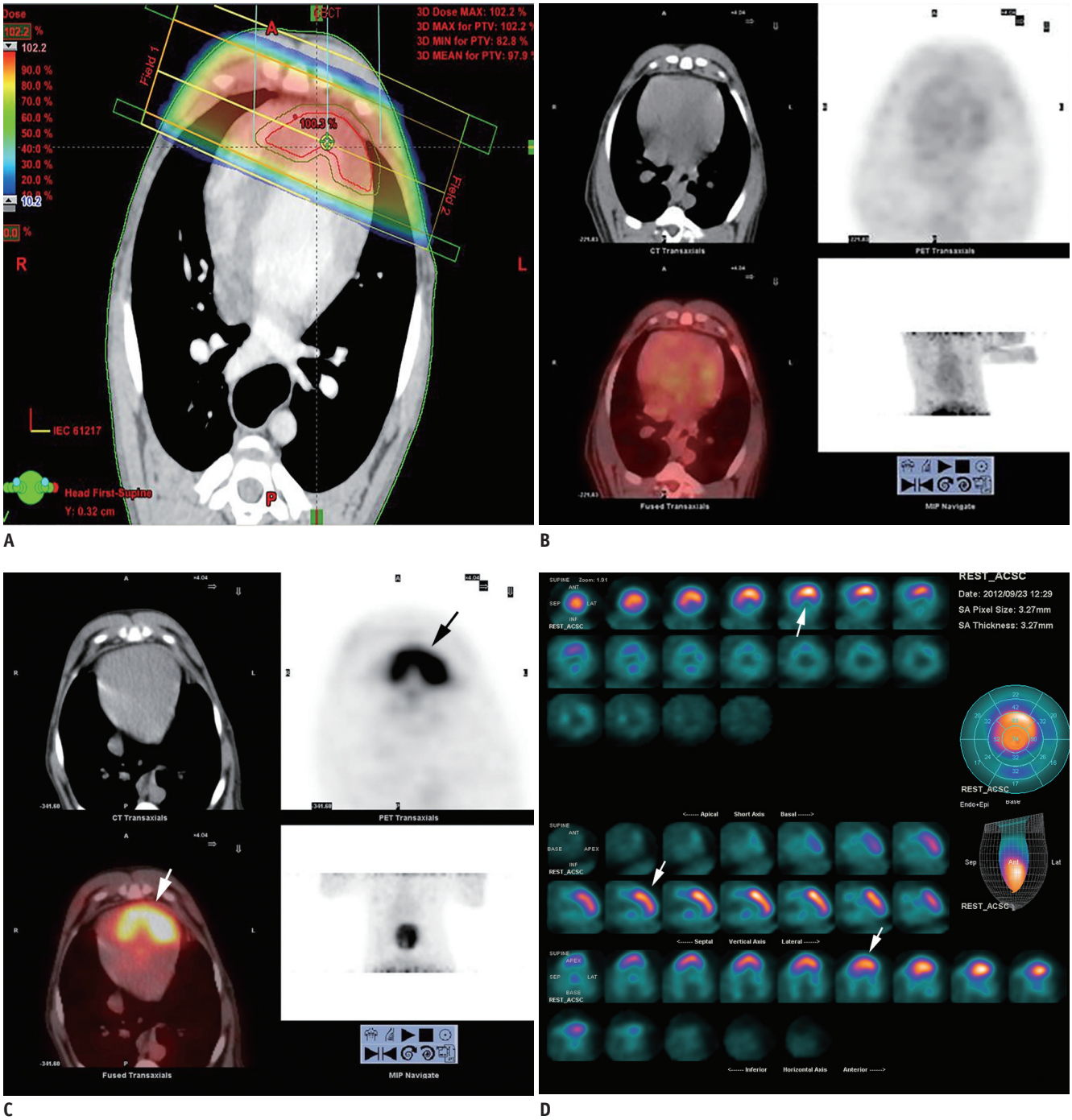

A B

C D

Fig. 3. Images of male beagle (M2) at baseline and 3 months after RT using F-HFD protocol.
A. Dose-distribution axial image. **B.** Cardiac FDG-PET/CT axial images before RT. **C.** Cardiac FDG-PET/CT axial images 3 months after RT. **D.** Myovation images of FDG at 3 months after RT. **B** shows suppression of myocardial FDG uptake before RT. **C** and **D** show high FDG uptake (arrows) corresponding to irradiated field 3 months after RT. FDG = fluorodeoxyglucose, F-HFD = fasting followed by a high-fat diet, PET/CT = positron emission tomography/computed tomography, RT = radiotherapy

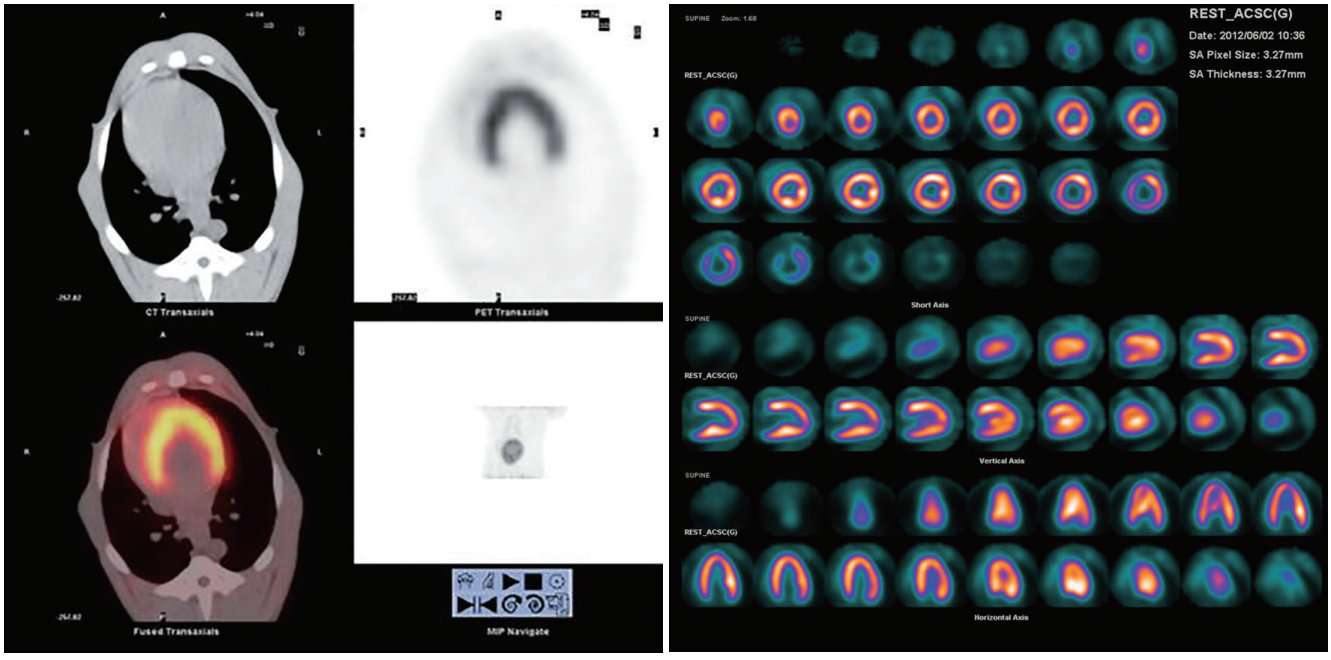

A B

Fig. 4. Images of bealge (M2) 3 months after RT under 12H-F protocol.
A. Cardiac FDG-PET/CT axial images 3 months after RT. **B.** Myovation images of FDG at 3 months after RT. No abnormal FDG uptake could be detected 3 months after RT. Physiological myocardial FDG uptake might interfere detecting pathological changes. 12H-F = 12 hours of fasting, FDG = fluorodeoxyglucose, PET/CT = positron emission tomography/computed tomography, RT = radiotherapy

Table 2. Comparison of Cases in Positive Findings with 12H-F and F-HFD Different Preparation Protocols

12H-F	F-HFD		Total
	+	-	
+	4	0	4
-	6	2	8
Total	10	2	12

Data are presented as number; McNemar test was used; *p* value was 0.031. 12H-F = 12-hour fasting before 18F-FDG tracer injection, 18F-FDG = 18F-fluorodeoxyglucose, F-HFD = 12-hour fasting followed by high fat diet and followed by another 3 hours before FDG tracer injection

and 2.54 ± 0.43, respectively ($p < 0.001$).

Echocardiography Results

Table 3 shows the results of left ventricular function parameters before and after RT. No difference was found between before and 3 months after RT in LVEDd, LVEDs, LVEF, and E/A.

Histological Changes

No morphological changes in the area outside of the irradiated field of the myocardium were found under H&E staining. However, all beagles displayed the myocardial damage in the irradiated field. The irradiated myocardium showed obvious perivascular fibrosis and mild myocardial degeneration and there was no inflammatory cell infiltration to the irradiated myocardium (Fig. 5).

Electron transmission micrographs showed a normal myocardium with abundant mitochondria packed around normal nuclei in the non-irradiated field. However, slightly dilated cristae in some mitochondria scattered around nuclei, as well as enlarged nuclei, were observed in the irradiated myocardium (Fig. 6).

DISCUSSION

Fasting may decrease insulin-dependent GLUT-4 reporters in myocytes to minimize myocardial 18F-FDG uptake, which has been the conventional preparation method for patients to perform oncological 18F-FDG PET/CT. However, we found variable and inconsistent 18F-FDG uptake of the myocardium under fasting conditions, consistent with previous reports (12, 13, 15). This is likely due to reduced levels of glucose and insulin in serum but also because of a low level of fatty acids in serum; thus, fasting may not be very effective for inhibiting physiological myocardial 18F-FDG uptake. Our results indicate that prescan protocol of fasting following an HFD may significantly inhibit physiological myocardial 18F-FDG uptake, a finding that is supported by other studies (14, 16, 17). The main reason for that might

Korean Journal of Radiology
KJR

be the Randle cycle (fatty acid-glucose cycle) in which fatty acid loading suppresses glucose metabolism (18). Furthermore, the F-HFD condition did not entail only adding an HFD, because the total fasting time for carbohydrates was 15 hours, 25% longer than that in the 12-Fr protocol. The effect of "long-term fasting" on myocardial 18F-FDG uptake has been controversial (12, 19, 20); however, the extended fasting that reduced glucose levels to minimize myocardial 18F-FDG uptake may have been of added value. Physiological uptake of 18F-FDG in cardiomyocytes will interfere with visualization by exhibiting abnormally high 18F-FDG uptake. Therefore, our study provides an effective and low-cost method to inhibit physiological myocardial 18F-FDG uptake.

The clinically conventional irradiation dose is 1.8–2.0 Gy per fraction, but the total dose is around 50 Gy. Krueger et al. (21) estimated that the mean heart dose was approximately 21 Gy, when the prescribed dose of breast RT is 50 Gy. Previous experimental studies have indicated that > 15 Gy is necessary to induce heart damage (22, 23). The ordinary dose used in these pre-clinical models of localized heart irradiation was either a single dose of 20 Gy or a fractionated sehedule of, for example, five daily fractions of 9 Gy (24). Therefore, we used a single 20 Gy for radiation in this study to reduce the experimental time and simplify the experimental procedure.

In the present study, focal increased 18F-FDG uptake was observed in the anterior myocardium corresponding to the irradiated field. In addition, the ratio of the irradiated field to the non-irradiated field SUV was significantly higher after irradiation than before irradiation. These findings are consistent with those of the previous clinical reports (9-11). However, this study was prospective rather than retrospective. In addition, the beagle model of regional heart irradiation was used, in which a clinically high dose of radiation to a small part of the heart, was simulated without clinical confounding factors, such as concurrent chemotherapy, and risk factors for cardiovascular disease. Furthermore, inhibition of physiological myocardial 18F-FDG uptake eliminated the negative interference on the diagnosis of pathological changes. Therefore, we explored that focal high myocardial 18F-FDG uptake in the irradiated

Table 3. Comparison of Echocardiography Parameters before (0 Month) and after (3 Months) RT

Parameters	0 Month	3 Months	*P*
LVEF (%)	69.2 ± 5.0	71.5 ± 7.4	0.398
LVEDd (mm)	31.3 ± 3.2	32.4 ± 3.1	0.418
LVEDs (mm)	19.9 ± 2.0	18.2 ± 3.9	0.236
E/A	1.87 ± 0.35	2.23 ± 0.11	0.449

Date are presented as mean ± standard deviations; paired Student's *t* test was used. A = transmitral late diastolic velocity, E = transmitral early diastolic velocity, LVEDd = left ventricular end-diastolic diameter, LVEDs = left ventricular end-systolic diameter, LVEF = left ventricular ejection fraction, RT = radiotherapy

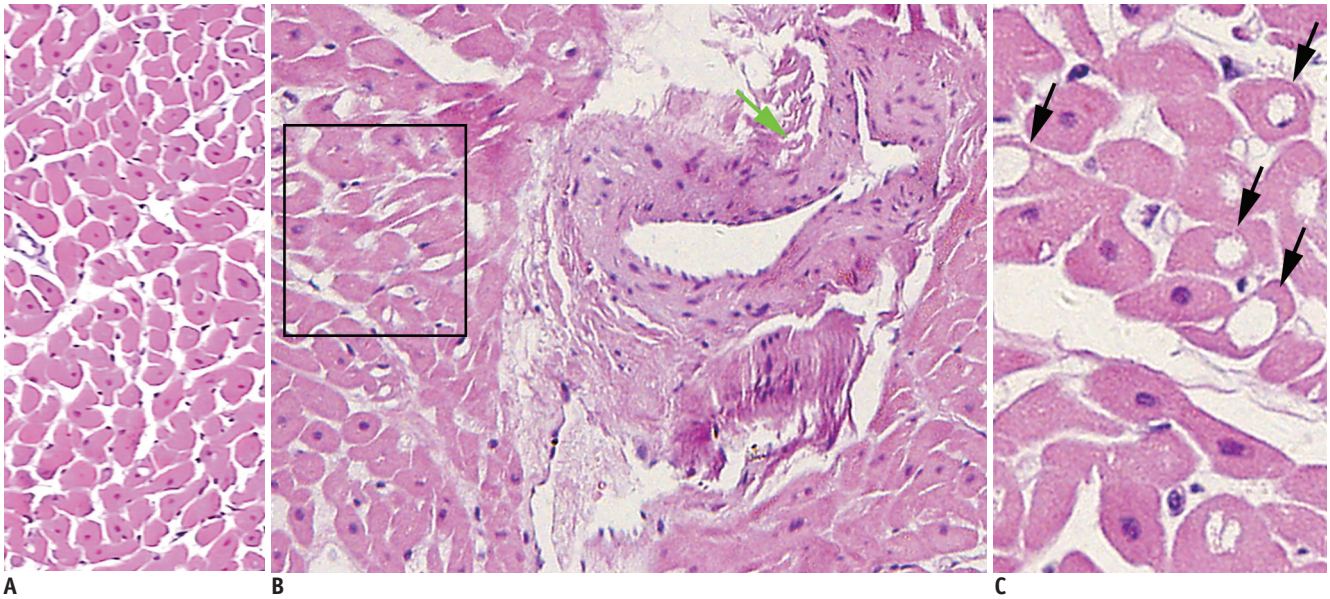

Fig. 5. Hematoxylin and esoin staining of non-irradiated myocardium (A) and irradiated myocardium (B, C).
Cytoplasmic vacuolization of myocytes (black arrows) (x 400) and perivascular fibrosis (green arrow) (x 200) were visible in irradiated field of myocardium.

field was related to radiation-induced myocardial damage.

Table 1 shows that the positive detection of RIHD using the F-HFD protocol was significantly higher than that using the 12H-F protocol, because there were some cases in which the myocardium 18F-FDG uptake showed a diffuse pattern, even under the condition of 12 hours of fasting. Such findings often decrease the sensitivity of detection of abnormally focal high uptake in the heart. However, the F-HFD protocol provides superior suppression of myocardial 18F-FDG uptake, thus offering better sensitivity for diagnosis of RIHD.

Because previous studies on this topic have all been clinical reports that did not obtain pathological tissue, the pathology of high myocardial 18F-FDG uptake in irradiated myocardium has remained unknown. In the present study, the irradiated myocardium showed obvious perivascular fibrosis and mild myocardial degeneration but little interstitial fibrosis. Yarnold and Brotons (25) demonstrated that radiation-induced myocardial damage is the direct effect of radiation of the endothelial cells of microvascular tissue. The main energy source of the myocardium changes from free fatty acids to glucose and lactate under ischemic conditions. In addition, Umezawa et al. (26) demonstrated reduced uptake metabolism of the myocardium within RT fields using I-123 BMIPP in patients who had completed RT for esophageal cancer. Therefore, these facts suggest that increased glucose metabolism might result from microvascular damage caused by radiation. Ischemia related coronary atherosclerosis may occur years after RT (27), whereas microvascular damage will occur after only a few months (28, 29). In addition, radiation alone may not induce atherosclerosis, but it may accelerate the atherosclerotic process (30, 31). However, we did not perform pathologic tests of the coronary arteries; the effect of irradiation of the coronary arteries needs further study. In the present study, we found no inflammatory cell infiltration (particularly macrophages) into the irradiated myocardium. Fajardo and Stewart (32) described that acute cellular infiltration to the myocardium, starting at 6 hours but disappearing by 48 hours after a single dose of 20 Gy irradiation to the hearts of rabbits. In the present study, our observation period was 3 months after irradiation with a single dose of 20 Gy. Therefore no inflammatory cells were found because of the time interval between irradiation and 18F-FDG PET/CT imaging, even if acute inflammation might have occurred in the irradiated hearts. Thus, we speculated that inflammatory cell infiltration may not participate in the mechanism of increased 18F-FDG uptake in irradiated myocardium. In ultrastructural evaluations, changes in mitochondrial vacuoles were observed. Barjaktarovic et al. (33) demonstrated that radiation-induced impairment of mitochondrial oxidative metabolism, which served as the

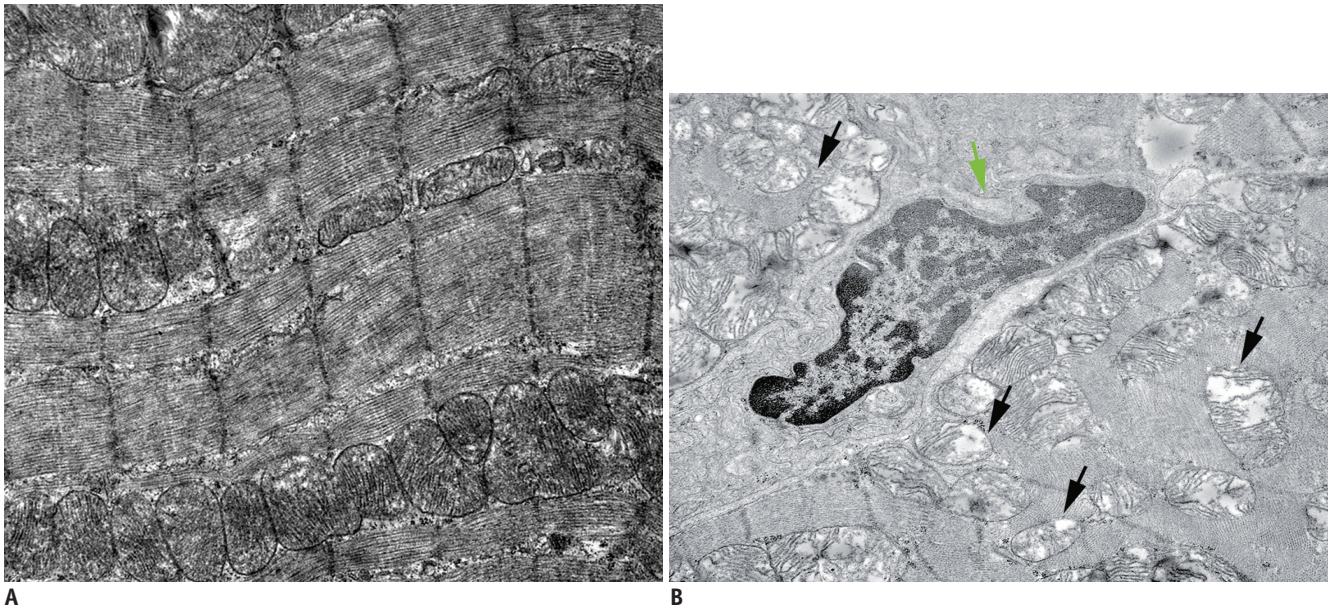

A B

Fig. 6. Electron transmission micrographs of myocardium.
A. Abundant mitochondria packed around normal nuclei are shown in non-irradiated field (x 10000). **B.** Slightly dilated cristae in some mitochondria scattered around nucleus (black arrows), as well as enlarged nuclei (green arrows) were observed in irradiated myocardium (x 10000).

Korean Journal of Radiology
KJR

first stage in etiology of RIHD. Consequently, changes in metabolism might also result from myocardial cell injury directly due to radiation.

In the present study, high 18F-FDG uptake in the irradiated field was observed as early as 3 months after irradiation. However, no cardiac dysfunction was found at 3 months after irradiation by echocardiography. Studies have demonstrated that radiation induces myocardial damage because of the direct effects of irradiation on the endothelial cells of microvascular tissue, causing myocardial ischemia, and ultimately leading to progressive myocardial fibrosis and functional changes (23, 25). The monitoring of cardiac function after chest RT by echocardiography is a routine technique to detect of RIHD, which is a late-stage event. At this stage, myocardial damage cannot be reversed, again highlighting the importance of early detection. In the present study, we found that focal high 18F-FDG uptake in the irradiated field was related with microvascular damage and mitochondrial injury, which were early stages of RIHD. Therefore, 18F-FDG PET/CT might have great value for early diagnosis of RIHD and provide a good opportunity for the early prevention and treatment of RIHD before irreversible pathology changes occur.

Dogan et al. (34) demonstrated that reduced rest myocardial perfusion occurred 6 months but not 4 months after radiation, in which a single dose of 20 Gy was irradiated to the whole heart of rats. Therefore, we inferred that abnormal 18F-FDG findings in the irradiated field might appear before perfusion defects. However, we did not perform a perfusion study at the same time as the control procedure; abnormal 18F-FDG findings before appearance of perfusion defects will require further extensive testing.

Perfusion defects in irradiated myocardium have been observed in some studies on myocardial perfusion imaging. Because myocardial perfusion imaging is limited to the evaluation of myocardial function, 18F-FDG PET/CT imaging that enables the evaluation of myocardial metabolism may have more clinical values for detecting RIHD. In addition, PET myocardial perfusion imaging has higher resolution, sensitivity, and specificity than single photon emission computed tomography imaging (35). Moreover, 18F-FDG PET/CT is an important noninvasive technique for follow-up after chemoradiotherapy for thoracic tumors. However, the limitation of 18F-FDG PET is that 18F-FDG uptake is occasionally observed in the whole myocardium. These findings often mimic abnormally high uptake in the heart.

This study had several limitations. First, there was no normal control group of animals without radiation and we included only a self control group before and after RT. However, this limitation did not influence our observation of the pathology and metabolism of radiation on the myocardium. In addition, 2 of 12 animals had a mild myocardial 18F-FDG uptake pattern under F-HFD. Further studies are needed to identify a more stable and reliable protocol to inhibit myocardial 18F-FDG uptake.

In conclusion, high myocardial 18F-FDG uptake in irradiated fields may be associated with radiation-induced myocardial damage, and related to myocardial ischemia resulting from microvascular damage by radiation and/or a change in metabolism caused by direct injury of the mitochondria by radiation. 18F-FDG PET/CT can detect early-stage of radiation-induced myocardial damage before abnormal cardiac function. The F-HFD preparation protocol before obtaining PET/CT imaging can improve the sensitivity for the diagnosis of RIHD.

Acknowledgments

We give special thanks for the technical support from the Institute of Radiation Protection in China.

REFERENCES

1. Favourable and unfavourable effects on long-term survival of radiotherapy for early breast cancer: an overview of the randomised trials. Early Breast Cancer Trialists' Collaborative Group. *Lancet* 2000;355:1757-1770
2. Aleman BM, van den Belt-Dusebout AW, De Bruin ML, van' t Veer MB, Baaijens MH, de Boer JP, et al. Late cardiotoxicity after treatment for Hodgkin lymphoma. *Blood* 2007;109:1878-1886
3. Lally BE, Detterbeck FC, Geiger AM, Thomas CR Jr, Machtay M, Miller AA, et al. The risk of death from heart disease in patients with nonsmall cell lung cancer who receive postoperative radiotherapy: analysis of the Surveillance, Epidemiology, and End Results database. *Cancer* 2007;110:911-917
4. Hardy D, Liu CC, Cormier JN, Xia R, Du XL. Cardiac toxicity in association with chemotherapy and radiation therapy in a large cohort of older patients with non-small-cell lung cancer. *Ann Oncol* 2010;21:1825-1833
5. Mukherjee S, Aston D, Minett M, Brewster AE, Crosby TD. The significance of cardiac doses received during chemoradiation of oesophageal and gastro-oesophageal junctional cancers. *Clin Oncol (R Coll Radiol)* 2003;15:115-120
6. Early Breast Cancer Trialists' Collaborative Group (EBCTCG), Darby S, McGale P, Correa C, Taylor C, Arriagada R, et al. Effect of radiotherapy after breast-conserving surgery on 10-year recurrence and 15-year breast cancer death: meta-analysis of

individual patient data for 10,801 women in 17 randomised trials. *Lancet* 2011;378:1707-1716
7. Clarke M, Collins R, Darby S, Davies C, Elphinstone P, Evans E, et al. Effects of radiotherapy and of differences in the extent of surgery for early breast cancer on local recurrence and 15-year survival: an overview of the randomised trials. *Lancet* 2005;366:2087-2106
8. Townsend DW, Carney JP, Yap JT, Hall NC. PET/CT today and tomorrow. *J Nucl Med* 2004;45 Suppl 1:4S-14S
9. Jingu K, Kaneta T, Nemoto K, Ichinose A, Oikawa M, Takai Y, et al. The utility of 18F-fluorodeoxyglucose positron emission tomography for early diagnosis of radiation-induced myocardial damage. *Int J Radiat Oncol Biol Phys* 2006;66:845-851
10. Zöphel K, Hölzel C, Dawel M, Hölscher T, Evers C, Kotzerke J. PET/CT demonstrates increased myocardial FDG uptake following irradiation therapy. *Eur J Nucl Med Mol Imaging* 2007;34:1322-1323
11. Unal K, Unlu M, Akdemir O, Akmansu M. 18F-FDG PET/CT findings of radiotherapy-related myocardial changes in patients with thoracic malignancies. *Nucl Med Commun* 2013;34:855-859
12. Inglese E, Leva L, Matheoud R, Sacchetti G, Secco C, Gandolfo P, et al. Spatial and temporal heterogeneity of regional myocardial uptake in patients without heart disease under fasting conditions on repeated whole-body 18F-FDG PET/CT. *J Nucl Med* 2007;48:1662-1669
13. Fragasso G, Lucignani G, Fazio F. Nonuniformity in myocardial accumulation of fluorine-18-fluorodeoxyglucose in normal fasted humans. *J Nucl Med* 1991;32:1832-1833
14. Williams G, Kolodny GM. Suppression of myocardial 18F-FDG uptake by preparing patients with a high-fat, low-carbohydrate diet. *AJR Am J Roentgenol* 2008;190:W151-W156
15. Fukuchi K, Ohta H, Matsumura K, Ishida Y. Benign variations and incidental abnormalities of myocardial FDG uptake in the fasting state as encountered during routine oncology positron emission tomography studies. *Br J Radiol* 2007;80:3-11
16. Kobayashi Y, Kumita S, Fukushima Y, Ishihara K, Suda M, Sakurai M. Significant suppression of myocardial (18) F-fluorodeoxyglucose uptake using 24-h carbohydrate restriction and a low-carbohydrate, high-fat diet. *J Cardiol* 2013;62:314-319
17. Harisankar CN, Mittal BR, Agrawal KL, Abrar ML, Bhattacharya A. Utility of high fat and low carbohydrate diet in suppressing myocardial FDG uptake. *J Nucl Cardiol* 2011;18:926-936
18. Frayn KN. The glucose-fatty acid cycle: a physiological perspective. *Biochem Soc Trans* 2003;31(Pt 6):1115-1119
19. Kaneta T, Hakamatsuka T, Takanami K, Yamada T, Takase K, Sato A, et al. Evaluation of the relationship between physiological FDG uptake in the heart and age, blood glucose level, fasting period, and hospitalization. *Ann Nucl Med* 2006;20:203-208
20. de Groot M, Meeuwis AP, Kok PJ, Corstens FH, Oyen WJ. Influence of blood glucose level, age and fasting period on non-pathological FDG uptake in heart and gut. *Eur J Nucl Med Mol Imaging* 2005;32:98-101
21. Krueger EA, Schipper MJ, Koelling T, Marsh RB, Butler JB, Pierce LJ. Cardiac chamber and coronary artery doses associated with postmastectomy radiotherapy techniques to the chest wall and regional nodes. *Int J Radiat Oncol Biol Phys* 2004;60:1195-1203
22. Schultz-Hector S, Trott KR. Radiation-induced cardiovascular diseases: is the epidemiologic evidence compatible with the radiobiologic data? *Int J Radiat Oncol Biol Phys* 2007;67:10-18
23. Lauk S, Kiszel Z, Buschmann J, Trott KR. Radiation-induced heart disease in rats. *Int J Radiat Oncol Biol Phys* 1985;11:801-808
24. Boerma M, Hauer-Jensen M. Preclinical research into basic mechanisms of radiation-induced heart disease. *Cardiol Res Pract* 2010;2011. http://dx.doi.org/10.4061/2011/858262
25. Yarnold J, Brotons MC. Pathogenetic mechanisms in radiation fibrosis. *Radiother Oncol* 2010;97:149-161
26. Umezawa R, Takase K, Jingu K, Takanami K, Ota H, Kaneta T, et al. Evaluation of radiation-induced myocardial damage using iodine-123 β-methyl-iodophenyl pentadecanoic acid scintigraphy. *J Radiat Res* 2013;54:880-889
27. Schultz-Hector S, Kallfass E, Sund M. [Radiation sequelae in the large arteries. A review of clinical and experimental data]. *Strahlenther Onkol* 1995;171:427-436
28. Lauk S, Trott KR. Endothelial cell proliferation in the rat heart following local heart irradiation. *Int J Radiat Biol* 1990;57:1017-1030
29. Schultz-Hector S. Experimental studies on the pathogenesis of damage in the heart. *Recent Results Cancer Res* 1993;130:145-156
30. Vos J, Aarnoudse MW, Dijk F, Lamberts HB. On the cellular origin and development of atheromatous plaques. A light and electron microscopic study of combined X-ray and hypercholesterolemia-induced atheromatosis in the carotid artery of the rabbit. *Virchows Arch B Cell Pathol Incl Mol Pathol* 1983;43:1-16
31. Shankar SM, Marina N, Hudson MM, Hodgson DC, Adams MJ, Landier W, et al. Monitoring for cardiovascular disease in survivors of childhood cancer: report from the Cardiovascular Disease Task Force of the Children's Oncology Group. *Pediatrics* 2008;121:e387-e396
32. Fajardo LF, Stewart JR. Experimental radiation-induced heart disease. I. Light microscopic studies. *Am J Pathol* 1970;59:299-316
33. Barjaktarovic Z, Schmaltz D, Shyla A, Azimzadeh O, Schulz S, Haagen J, et al. Radiation-induced signaling results in mitochondrial impairment in mouse heart at 4 weeks after exposure to X-rays. *PLoS One* 2011;6:e27811
34. Dogan I, Sezen O, Sonmez B, Zengin AY, Yenilmez E, Yulug E, et al. Myocardial perfusion alterations observed months after radiotherapy are related to the cellular damage. *Nuklearmedizin* 2010;49:209-215
35. Bateman TM. Advantages and disadvantages of PET and SPECT in a busy clinical practice. *J Nucl Cardiol* 2012;19 Suppl 1:S3-S11